Supporting Information

Nanoelectronic Discrimination of Non-malignant and Malignant Cells using Nanotube Field-Effect Transistors

Guilherme O. Silva,[‡a,b] Zachary P. Michael,[‡a] Long Bian,[a] Galina V. Shurin,[c] Marcelo Mulato,[b] Michael R. Shurin,[c] and Alexander Star*[a]

[a] Department of Chemistry, University of Pittsburgh, 219 Parkman Avenue, Pittsburgh, PA 15260 (USA)

[b] Department of Physics, Faculty of Philosophy, Science and Letters at Ribeirão Preto, University of São Paulo, Avenida Bandeirantes 3900, Ribeirão Preto, São Paulo 14040-401 (Brazil)

[c] Department of Pathology, University of Pittsburgh Medical Center, 3550 Terrace Street, Pittsburgh, PA 15261 (USA)

Table of Contents

Experimental Procedures

1. Chemicals

Commercially available SWCNTs were acquired from Carbon Solutions, Inc. Polydimethyl siloxane (PDMS) was purchased from Ellsworth Adhesives. The metal salts $HAuCl_4$ (99.9%), H_2PtCl_6 (99.9%), Na_3RhCl_6 (Mw: 384.59 $g \cdot mol^{-1}$), $Pd(Ac)_2$ (98%), and the tastants: anhydrous caffeine ($C_8H_{10}N_4O_2$), L-glucose ($C_6H_{12}O_2$), L-glutamic acid monosodium salt monohydrate ($C_5H_8NNaO_4 \cdot xH_2O$, 169.11 $g \cdot mol^{-1}$) and lipoic acid were procured from Sigma Aldrich. Dodecanethiol and sodium chloride (NaCl) were purchased from Fisher Scientific. All other reagents were analytical grade. Nanopure water from Thermo Scientific Barnstead Nanopure System with resistivity >18.2 MΩ·cm was used to prepare all solutions.

2. Carbon nanotube preparation

SWCNTs were oxidized according to previously published procedure.[S1] Briefly, SWCNTs were oxidized using a mixture of concentrated H_2SO_4:HNO_3 (3:1) for two hours in a bath sonicator to generate a variety of oxygenated defect sites. These oxidized SWCNTs were filtered and rinsed thoroughly with nanopure water to remove excess acid. The resulting material was suspended in nanopure water for further usage.

3. NTFETs assembly and decoration with metal nanoparticles

Si wafers consisting of four interdigitated gold electrode devices were fabricated *via* a standard photolithography process (Figure 1a). These 2x2 mm chips were then wirebonded into standard 40-pin ceramic dual in-line packages (CerDIP) and secured with PDMS to protect and passivate the electrical contacts. Liquid wells were fixed to the packages using PDMS for incubation with self-assembled monolayer (SAM) precursors and analyzed solutions. SWCNTs were integrated between electrodes using AC dielectrophoretic (DEP) deposition (0.01 mg/mL SWCNT in water, 10 V_{pp} at 10 MHz for 60 s). Metal nanoparticles (MNPs: Au, Pt, Rh, Pd) were then introduced through bulk electrolysis using a CH Instruments electrochemical analyzer in a three-system electrode setup (Ag/AgCl as reference, Pt as counter, and SWCNT as working electrodes) from a metal solution at 1 mM in 0.1 M HCl).[S2] Size of MNPs was optimized for these experiments through control of deposition voltage (-0.2 V) and time (20 s). This process results in discrete MNPs in sizes ranging from 10-100 nm anchored to defect sites of the oxidized SWCNTs.

4. Functionalization of AuNPs with SAMs

Dodecanethiol[S3] and lipoic acid[S4] were prepared in 1:1 EtOH:H_2O and EtOH at 10 mM, respectively. 200 µL of the desired monolayer precursors molecule was added to the chip surface and the liquid well was sealed with parafilm. Monolayer formation was allowed to occur over a 24-hour time period, after which the chips were thoroughly rinsed with EtOH and blown dry with N_2 for further experiments.

5. Preparation of cell samples

Mouse tumor cell lines B16 melanoma, 3LL Lewis lung carcinoma, and EL4 T cell lymphoma were obtained from ATTC and cultured in RPMI 1640 medium (GIBCO BRL) supplemented with non-essential amino acids, 10% heat-inactivated FBS, 2 mM L-glutamine, 100 $IUml^{-1}$ penicillin and 100 μgml^{-1} streptomycin (Invitrogen Life Technologies Inc.). Bone marrow, spleen, lung, skin, and liver specimens were harvested from C57BL/6 mice (Taconic)) and used for preparation of single cell suspensions. Bone marrow cells were collected from tibia, resuspended, separated on nylon cell strainer and washed in RPMI 1640 medium. Bone marrow cells were also treated with monensin (BioLegend) (0.2 mM, 4 h in RPMI 1640 medium) to block exocytosis. Splenocytes were prepared from minced spleens using frosted microscope slides, resuspended and washed in RPMI 1640 medium. Lung and liver tissues were enzymatically digested with DNAse and Collagenase type IV (Worthington) (45 min, RPMI 1640 medium) and washed. Skin was minced and digested with Dispase type II, trypsin, and Collagenase type IV (Roche). All cell suspensions were finally washed in PBS and cell numbers were determined on automatic cell counter (Logos Biosystems).

6. NTFET electrical characterization

NTFET transfer characteristics were recorded by introducing the desired solution into the liquid well and addressing the device with a Ag/AgCl reference electrode (CHI111, CH Instruments, Inc). Gate voltage was swept from +0.6 V to -0.6 V with a constant 50 mV source-drain voltage and source-drain current recorded as a function of gate voltage using two Keithley 2400. For tastants experiments NTFET transfer characteristics were collected from each device type in nanopure water as a baseline. Subsequently, tastant solutions at 1 mM (NaCl for saltiness, glucose for sweetness, citric acid for sourness, caffeine for bitterness and glutamic acid for umami) were

introduced to the chip surface and allowed to incubate for 5 minutes to reach adsorption equilibrium. Thereafter, a second curve was collected. For cell experiments, NFFET characteristics were collected from each device type in PBS at 1 mM as baseline. Subsequently, cell samples in PBS at 10^6 cells mL^{-1} were then introduced to the liquid well and allowed to incubate at room temperature for an hour. After the elapsed period time, a second NTFET transfer characteristics recorder as previously.

7. Calculation of FET characteristic responses

Characteristic (1): Transconductance of the device was calculated as the slope, t, of the linear region of FET devices (dashed lines in Figure 1b). Relative response was calculated as:

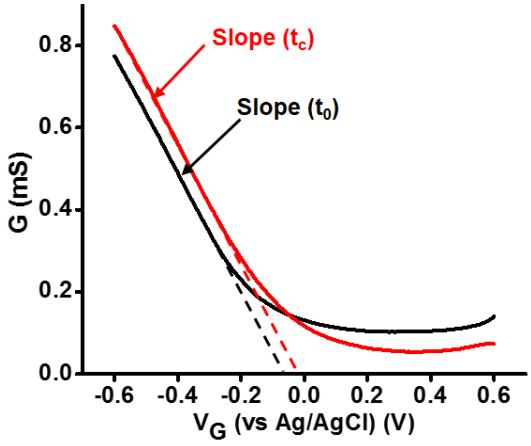

$$(t_c - t_0)/t_0$$

Characteristic (2): Threshold voltage was calculated using the second derivative method.[S5] Briefly, the second derivative of the conductance was taken with respect to gate voltage and maximum $\partial^2 G/\partial V_g^2$ was found. V_g at this value is the threshold voltage (V_{th}). Response was calculated as:

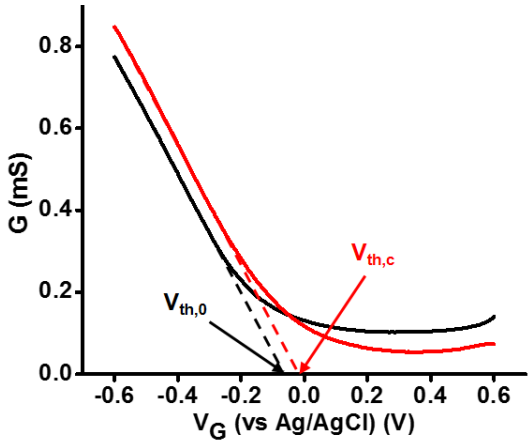

$$V_{th,c} - V_{th,0}$$

Characteristics (3 and 10): Conductance values at V_g = ±0.6 V were found and relative response calculated as:

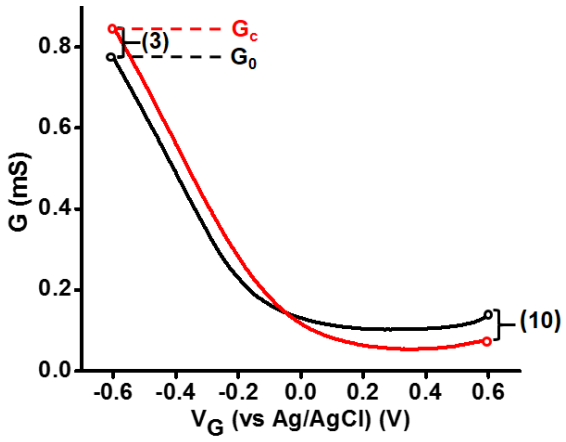

$$(G_c - G_0)/G_0$$

Characteristics (4 to 9): Conductance values at V_g = ± 0.6, 0.4, and 0.3 V were found. Conductance at the threshold voltage of the initial curve was found. Normalized response was calculated as:

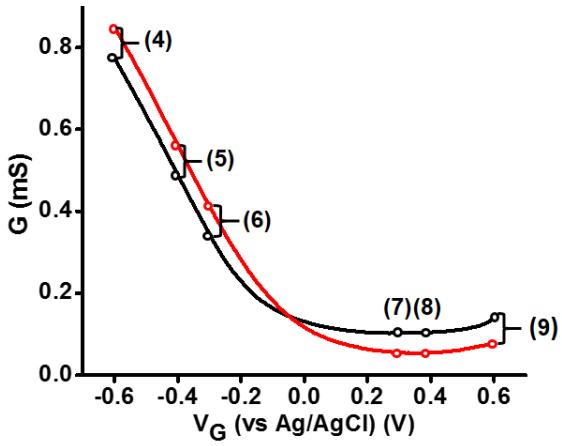

$$(G_c - G_0)/G_{0@Vth}$$

Characteristic (11): Minimum conductance of the device was found. Relative response was calculated as:

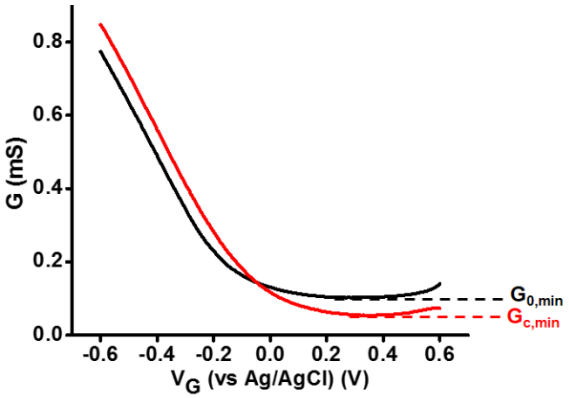

$$(G_{c,min} - G_{0,min})/G_{0,min}$$

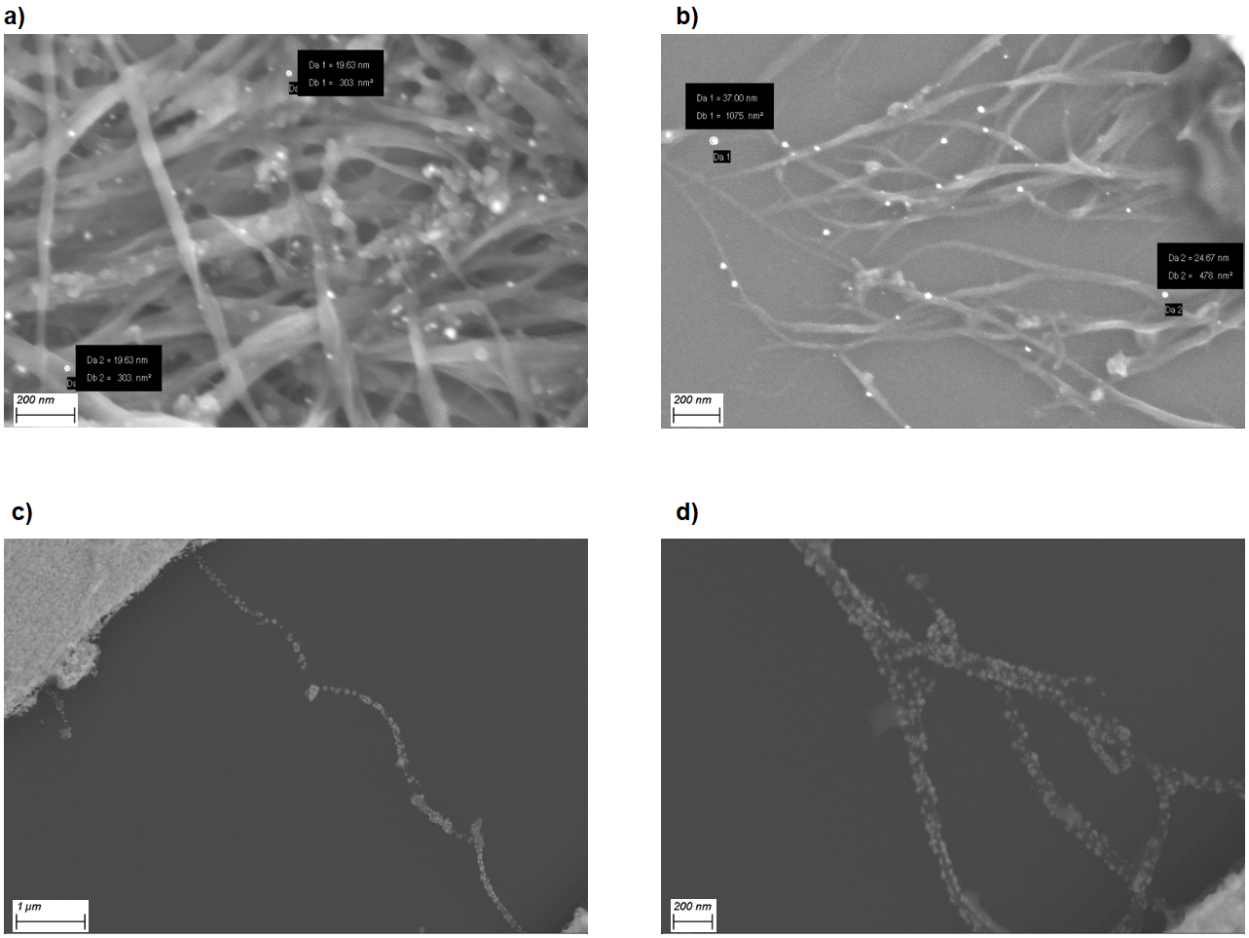

Figure S1. Scanning Electron Microscopy (SEM) micrographs of networks of single-walled carbon nanotubes (SWCNTs) decorated with metal nanoparticles. Platinum nanoparticles a) and b). Palladium nanoparticles c) and d).

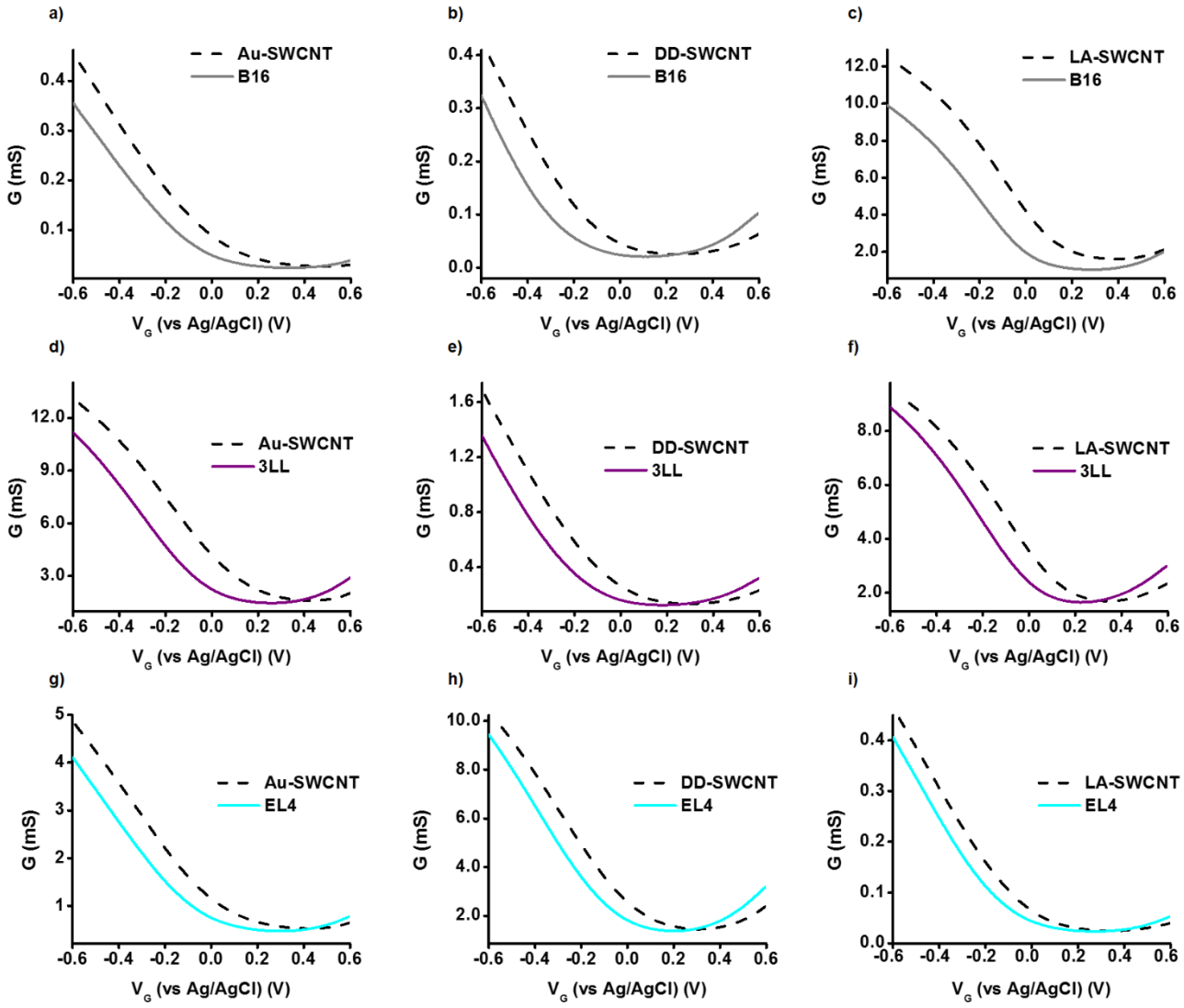

Figure S2. FET characteristic curves of tumor cell lines. Curves for Au-SWCNT (left column), DD-SWCNT (middle column), and LA-SWCNT (right column) and their response to B16 melanoma (gray lines, a-c), 3LL lung carcinoma (purple lines, d-f) and EL4 lymphoma (cyan lines, g-i).

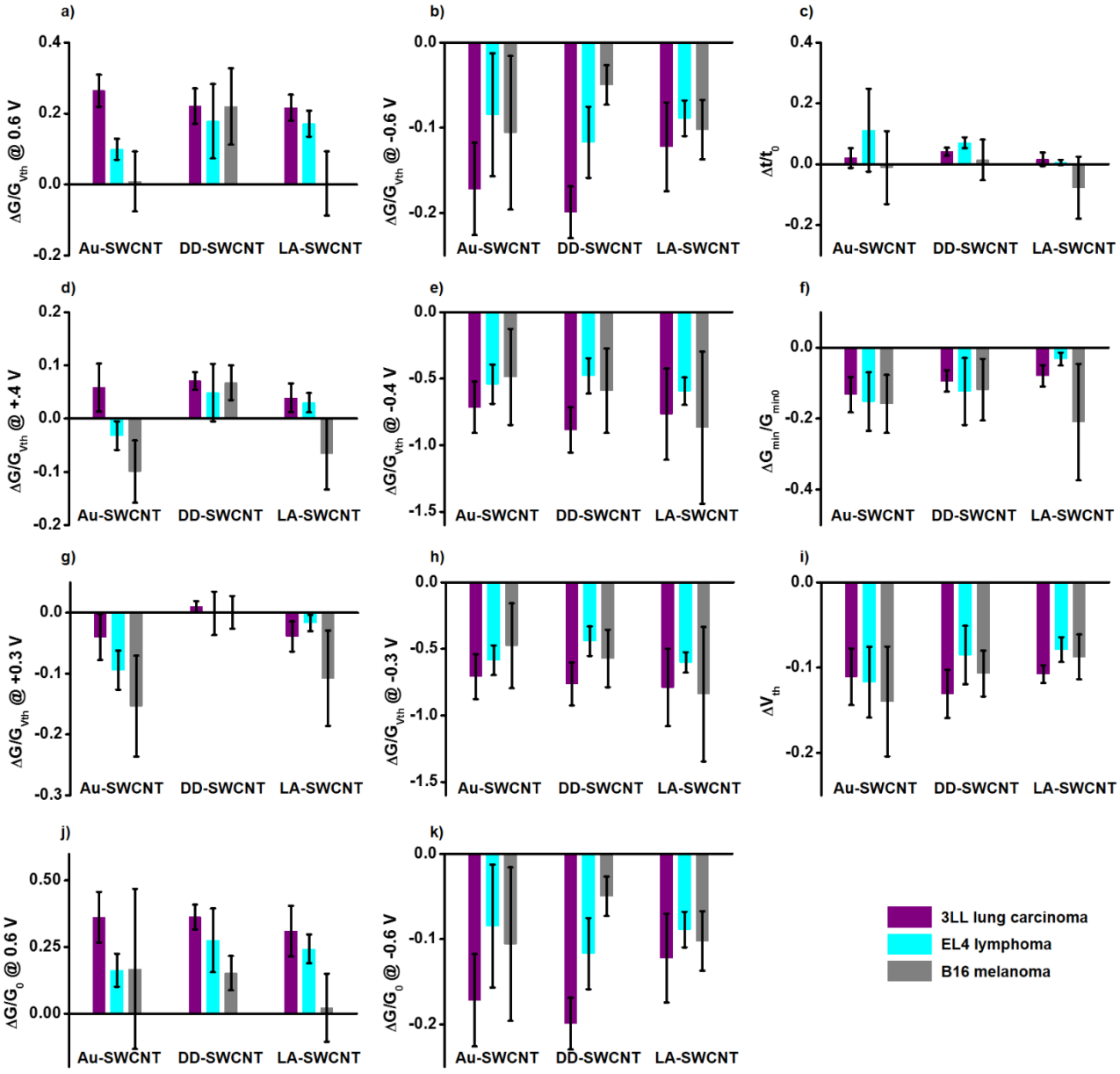

Figure S3. Average response of Au-SWCNT, DD-SWCNT, and LA-SWCNT to 3LL lung carcinoma (purple), EL4 lymphoma (cyan), and B16 melanoma (gray) cell lines for the eleven FET characteristics. Error bars represent one standard deviation.

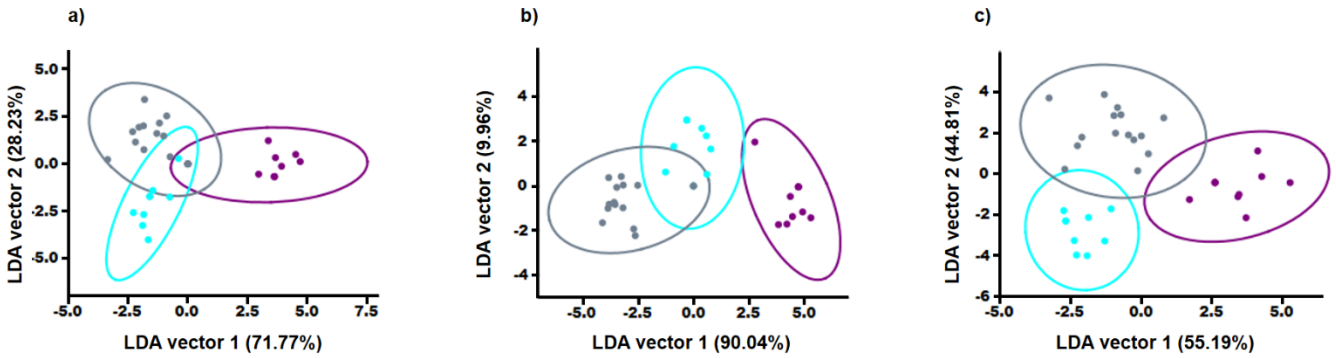

Figure S4. LDA results of tumor cell lines using single device functionalization: (a) Au-SWCNT, (b) DD-SWCNT, and (c) LA-SWCNT. B16 melanoma (gray), 3LL lung carcinoma (purple), and EL4 lymphoma (cyan). Ellipses represent 95% confidence intervals.

Table S1. Confusion matrices for LDA performed in Figure S4. Left: Au-SWCNT, middle: DD-SWCNT, right: LA-SWCNT.

	ELL	EL4	B16	Total		ELL	EL4	B16	Total		ELL	EL4	B16	Total
3LL	9	0	1	10	3LL	9	1	0	10	3LL	10	0	0	10
EL4	0	8	1	9	EL4	0	9	0	9	EL4	0	9	0	9
B16	0	0	15	15	B16	0	2	13	15	B16	0	0	15	15
total	9	8	17	34	Total	9	12	13	34	total	10	9	15	34

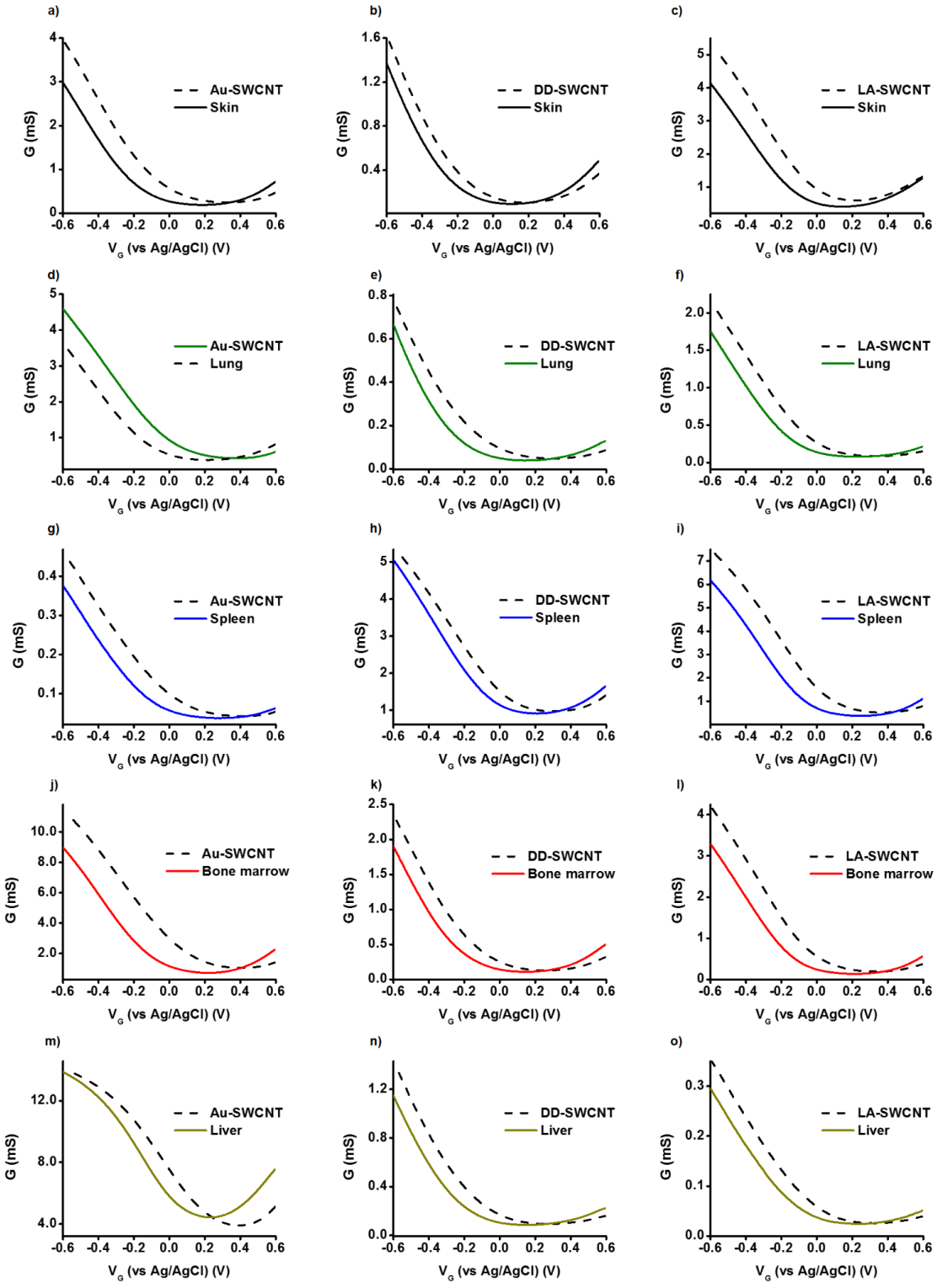

Figure S5. FET characteristic curves of murine healthy tissues**.** Curves for Au-SWCNT (left column), DD-SWCNT (middle column), and LA-SWCNT (right column) and their response to Skin cells (black lines, a, b, and c), Lung cells (green lines, d, e, and f), Spleen cells (blue lines, g, h, and i), bone marrow cells (red lines, j, k, and l), and liver cells (golden lines, m, n, and o).

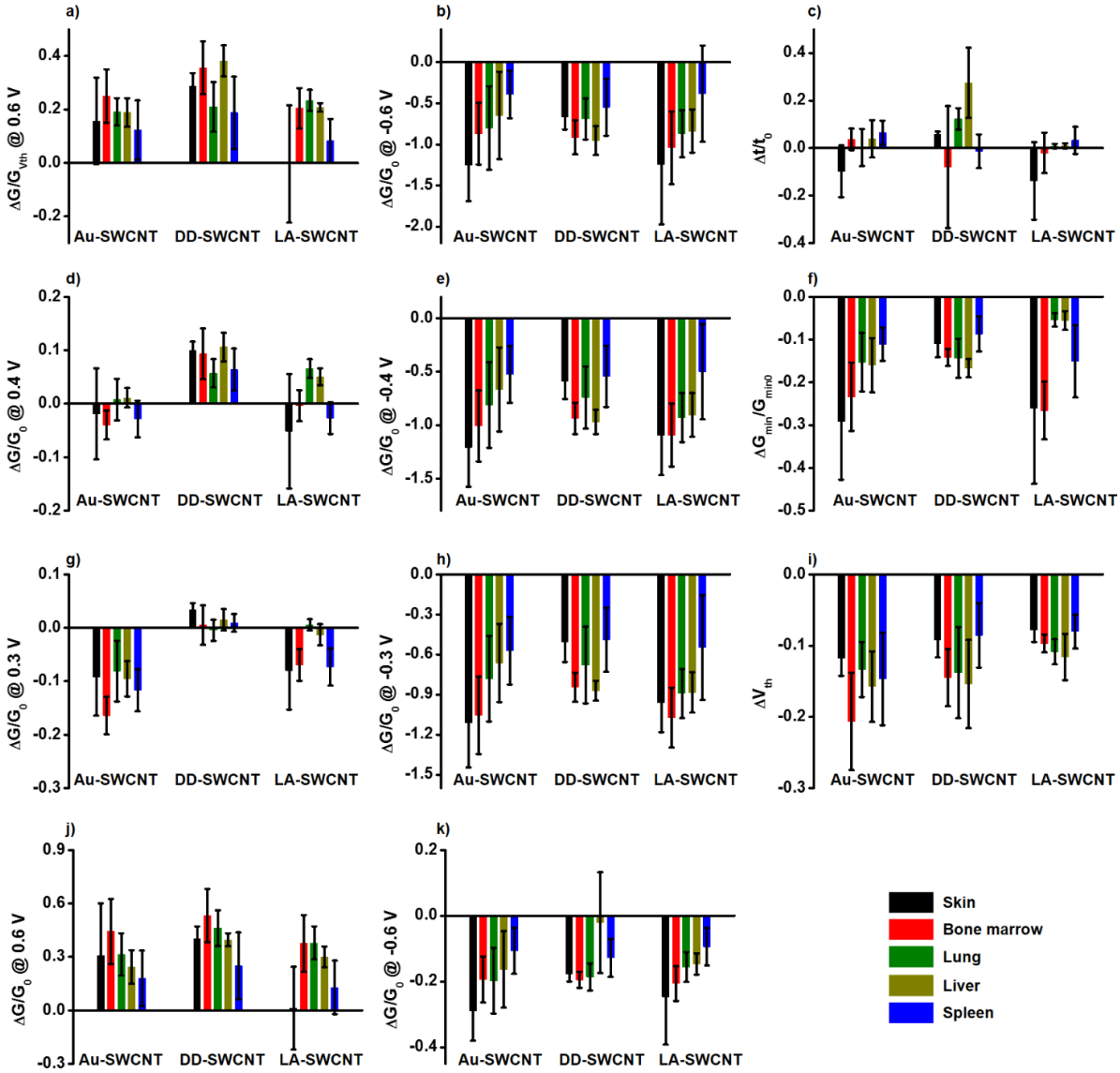

Figure S6. Average response of Au-SWCNT, DD-SWCNT, and LA-SWCNT to skin (black), bone marrow (red), lung (green), liver (golden), and spleen (blue) healthy murine tissue cells. Error bars represent one standard deviation.

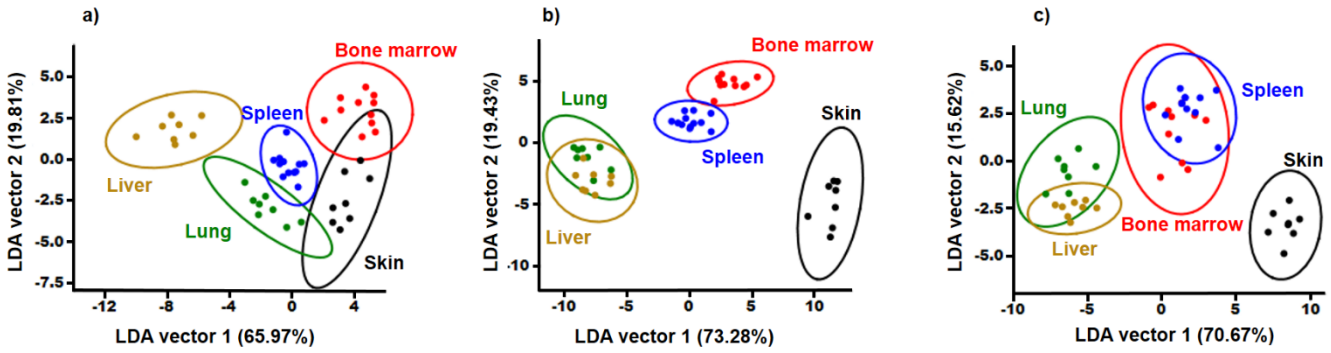

Figure S7. LDA results of murine tissue cells using two device functionalizations. a) Au-SWCNT and DD-SWCNT. b) Au-SWCNT and LA-SWCNT. c) DD-SWCNT and LA-SWCNT response to skin (black), bone marrow (red), lung (green), liver (golden), and spleen (blue). Ellipses represent 95% confidence intervals.

Table S2. Confusion matrix for LDA performed in Figure S7a.

	Skin	Bone Marrow	Lung	Liver	Spleen	Total
Skin	8	0	0	0	0	8
Bone Marrow	0	11	0	0	0	11
Lung	0	0	8	0	0	8
Liver	0	0	0	8	0	8
Spleen	0	0	0	0	12	12
total	8	11	8	8	12	47

Table S3. Confusion matrix for LDA performed in Figure S7b.

	Skin	Bone Marrow	Lung	Liver	Spleen	Total
Skin	8	0	0	0	0	8
Bone Marrow	0	11	0	0	0	11
Lung	0	0	7	1	0	8
Liver	0	0	1	7	0	8
Spleen	0	0	0	0	12	12
total	8	11	8	8	12	47

Table S4. Confusion matrix for LDA performed in Figure S7c.

	Skin	Bone Marrow	Lung	Liver	Spleen	Total
Skin	8	0	0	0	0	8
Bone Marrow	0	11	0	0	0	11
Lung	0	0	8	0	0	8
Liver	0	0	0	8	0	8
Spleen	0	0	0	0	12	12
total	8	11	8	8	12	47

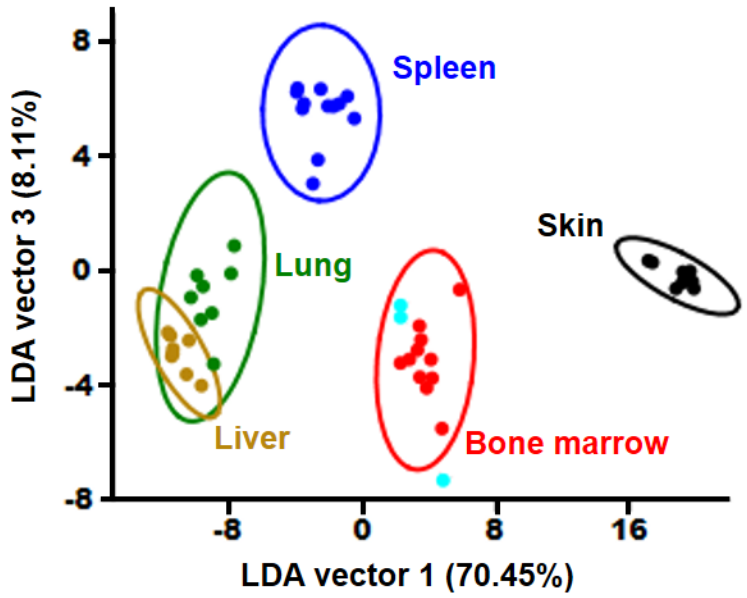

Figure S8. LDA response of murine tissue cell samples along with an unknown sample. The unknown sample (cyan) was identified as bone marrow cells (red). Ellipses represent 95% confidence intervals.

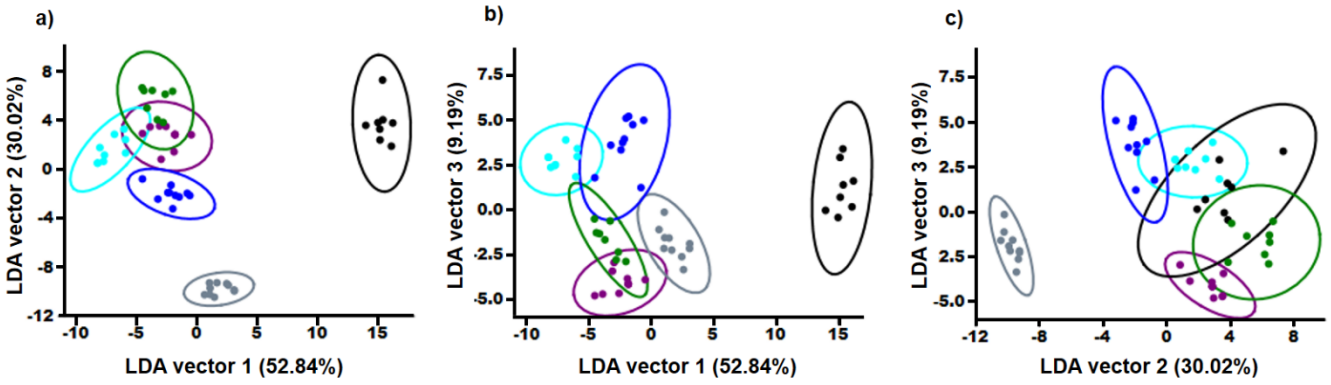

Figure S9. LDA results of healthy murine cells and their malignant counterparts lines: skin (black) and B16 melanoma (gray), spleen (blue) and EL4 lymphoma (cyan), lung (green) and 3LL carcinoma (purple). a) First and second canonical vectors. b) First and third canonical vectors. c) Second and third canonical vectors.

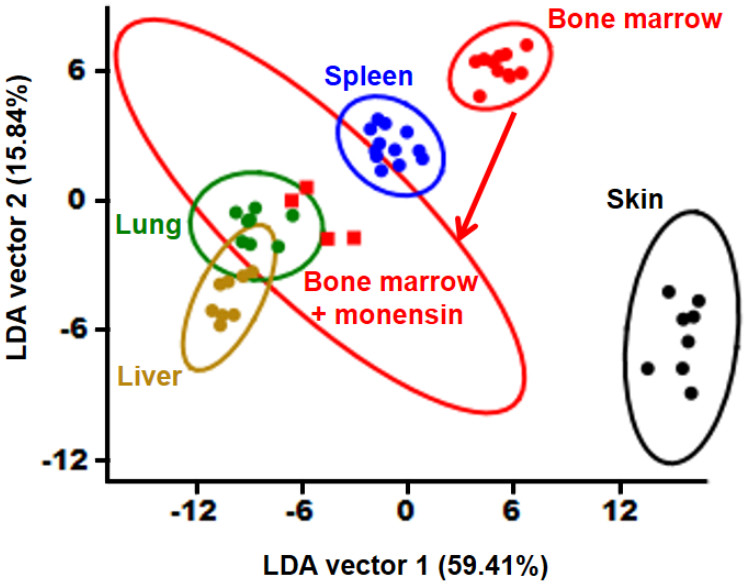

Figure S10. LDA of Au-SWCNT, DD-SWCNT, and LA-SWCNT response to murine tissue cell samples along with monensin-treated bone marrow cells. Large shift in data indicates a significant change in the sensor response to bone marrow cells, indicating extracellular components of tissue cell samples play an important role in distinct sensor responses. Ellipses represent 95% confidence intervals.

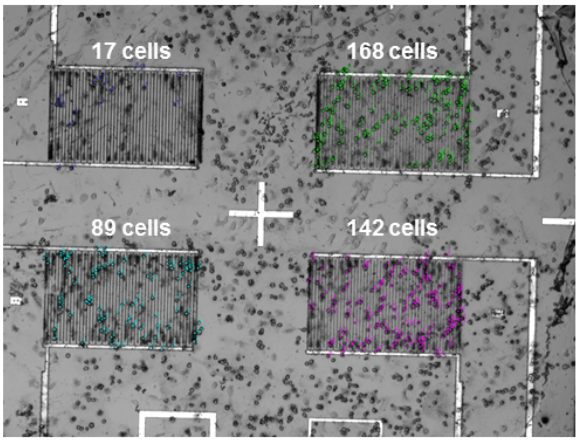

Figure S11. Optical image of bone marrow cells on Au-SWCNT. Cells were counted manually using ImageJ, highlighted by markers.

References

(S1) Gou, P.; Kraut, N. D.; Feigel, I. M.; Bai, H.; Morgan, G. J.; Chen, Y.; Tang, Y.; Bocan, K.; Stachel, J.; Berger, L.; *et al.* Carbon Nanotube Chemiresistor for Wireless pH Sensing. *Sci. Rep.* **2014**, *4*, 4468.

(S2) Day, T. M.; Unwin, P. R.; Wilson, N. R.; Macpherson, J. V. Electrochemical Templating of Metal Nanoparticles and Nanowireson Single-Walled Carbon Nanotube Networks. *J. Am. Chem. Soc.* **2005**, *127*, 10639–10647.

(S3) Dai, J.; Li, Z.; Jin, J.; Cheng, J.; Kong, J.; Bi, S. Study of the Solvent Effect on the Quality of Dodecanethiol Self-Assembled Monolayers on Polycrystalline Gold. *J. Electroanal. Chem.* **2008**, *624*, 315–322.

(S4) Vokert, A.; Subramaniam, V.; Ivanov, M.; Goodman, A.; Haes, A. Salt-Mediated Self Assembly of Thioctic Acid on Gold Nanoparticles. *ACS Nano* **2011**, *5*, 25–41.

(S5) Ortiz-Conde, A.; García-Sánchez, F. J.; Muci, J.; Terán Barrios, A.; Liou, J. J.; Ho, C. S. Revisiting MOSFET Threshold Voltage Extraction Methods. *Microelectron. Reliab.* **2013**, *53*, 90–104.